The Free Energy of Nanobubbles in Organic Liquids

Siegfried Höfinger* and Francesco Zerbetto*

Dipartimento di Chimica "G. Ciamician", Università di Bologna, V. F. Selmi 2, 40126 Bologna, Italy

Received: August 12, 2003; In Final Form: September 26, 2003

The free energy of formation of molecular-size cavities, ΔG_{cav}, in 12 organic liquids of common use as solvents is obtained from free energy perturbation simulations. They are acetone, cyclohexane, ethanol, toluene, chlorobenzene, benzene, tetrachloromethane, dichloromethane, chloroform, mesitylene, *o*-xylene, and tetrahydrofuran. The results are (1) cast in a simple way that should lead to an improvement over the most commonly used Pierotti equation for the calculation of ΔG_{cav} in quantum chemical computer programs and (2) used for assessing the relative contribution of cavitation free energy to the total solvation free energy in a set of nearly 100 solvent/solute pairs.

Introduction

The energy required to create a void inside an equilibrated liquid is called cavitation energy, ΔG_{cav}, and is of crucial importance in solvation phenomena. Solvation, in fact, may be formally divided in a step that forms a cavity by displacing the solvent, and a subsequent step that introduces the repulsive and attractive intermolecular forces at the solute−solvent interface. While continuum electrostatics and/or intermolecular interactions may be advocated to evaluate the energy of the second step, the initial process of forming a cavity poses a great challenge. One of the difficulties is that there is no practical way of determining ΔG_{cav} from experiments, since the ideal cavity requires a perfectly empty interior, something "hard" to achieve in a lab. At the nano- or subnanometer level, the analytical model of the Pierotti equation, PE,[1] has found widespread use in quantum chemical programs to calculate the energy that describes the displacement of the solvent to make room for a solute. An alternative simple approach applied in solvation models has been to use surface tension data.[2]

The important issues of solvation effects and hydrophobicity have received important contributions from a number of researchers such as Pohorille and Pratt,[3] Hummer and co-workers,[4] Ashbaugh and Paulaitis,[5] and Floris and co-workers,[6] to name only a few. One of the simplest ways to calculate ΔG_{cav} was devised by Pohorille and Pratt.[3] They focused on the evaluation of the statistical occurrence of transient cavities (limited in size) obtained from straightforward molecular dynamics simulations (MD) or Monte Carlo simulations (MC). The calculations provided a basis for deriving probability distributions for the solvent molecules to enter a certain volume. The probability of finding no solvent molecules in a certain region (transient cavity) was related to the chemical potential of a hard-sphere solute dissolved in the solvent. This approach is limited to small cavities and depends on the choice of model parameters used for the description of the solvent (see, Figure 3 and Figure 6 of ref. 3a, two different models used for water). Extension toward larger cavities was obtained through the observation that the probability distribution of having *n* solvent molecules in a given confined volume is a quasi-parabolic function, which may be further parameterized from information theory models.[4] The extrapolation to the zero-solvent-molecule probability connects the simulation data with actual cavitation free energies.

Another interesting distinction concerning dewetting and rewetting in the first hydration shell of solutes has been described by Ashbaugh and Paulaitits.[5] Free energy perturbation, FEP, calculations have already been recommended by Floris and co-workers in order to provide an accurate way of estimating the cavitation energy.[6] In that study MC was used and cavities up to a hard sphere radius of 5 Å were analyzed. Despite the finding of a convincing correlation between scaled particle theory and free energy perturbation results, critical were the choice of an appropriate hard sphere radius for the solvent and the definition of the relationship between soft-sphere radii and the corresponding hard-sphere values.

ΔG_{cav} can also be calculated by molecular dynamics, MD. Postma et al.[7] were the first to compare the results of PE with those of free energy perturbation. Very recently,[8] we used MD/FEP to calculate ΔG_{cav} for up to seven cavities in water and found good agreement with Postma (which implicitly proves that the results are not a strong function of the parameters used to describe water). We further found that in the region of the small radii considered, < 3Å, the free energy of cavity formation of nonspherical systems may be obtained from the volume-equivalent spherical one. This agrees with the intuitive notion that, at least for very small bubbles, the free energy scales with the number of molecules that are displaced to make the hole.

Here, in the same spirit, we report the treatment of 12 liquids (acetone, **1**, cyclohexane, **2**, ethanol, **3**, toluene, **4**, chlorobenzene, **5**, benzene, **6**, tetrachloromethane, **7**, dichloromethane, **8**, chloroform, **9**, mesitylene, **10**, *o*-xylene, **11**, tetrahydrofuran, **12**) that are of common use as solvents. Comparison is then given with the results of PE and surface tension data. The intent is not of superseding previous work that has shown the improvements that can be had over PE, something already discussed long time ago,[9] but of providing an estimate of the inaccuracy of the ΔG_{cav} calculated in this way by a number of quantum chemical programs.

Computational Background

The simulations were run with the TINKER 3.9 program,[10] which has found several satisfactory applications in our laboratory,[11] in conjunction with the MM3 force field.[12] The box size

* Corresponding authors. E-mail gatto@ciam.unibo.it; fax +39 051 2099456.

10.1021/jp036392o CCC: $25.00
Published on Web 11/15/2003

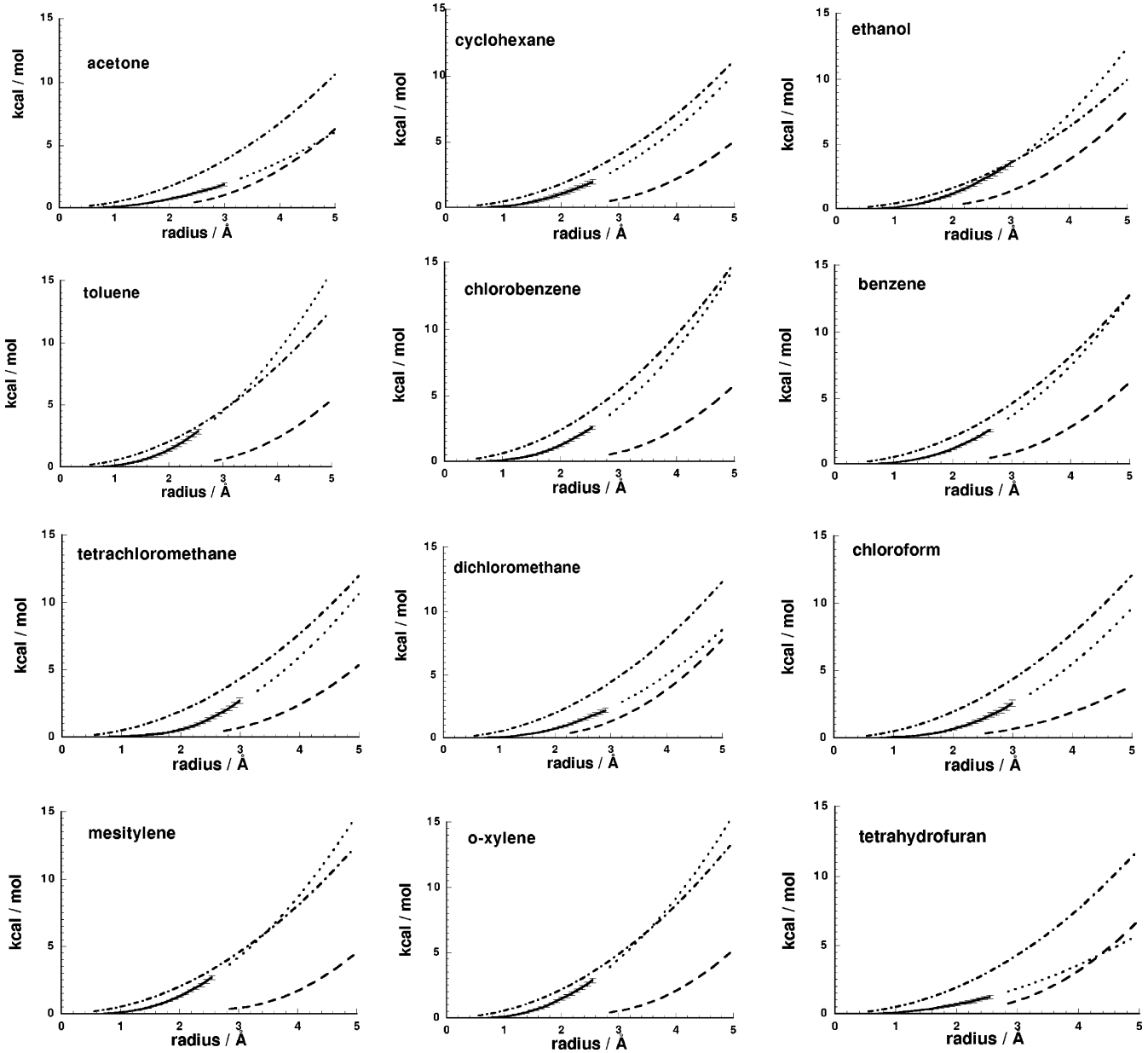

Figure 1. Free energy of cavity formation of twelve organic solvents: solid line is present FEP, dotted line its extrapolation, dashed line PE, dashed−dotted line is obtained from surface tension.

was dimensioned to reproduce the experimental density at $T =$ 300 K. Changes of the size of the box occur because of the variation of the cavity radius and the pressure coupling. Internal degrees of freedom, apart from CH stretches, were allowed to relax. Trajectories were calculated for 100 ps with a time step of 1.0 fs; the first 20 ps were used for equilibration. About 15 years of CPU time on a single MIPS R12000/400 MHz were required.

To create the cavity, a potential of the type

$$V_c = \lambda\left(\frac{B}{r}\right)^{12} \tag{1}$$

was introduced at the center of the box with 216 molecules. B defines the cavity radius, and all the intermediate cavity radii B_i correspond to a well-defined value of $0 < \lambda < = 1$. As the cavity repulsive radius tends to zero, the potential introduces a discontinuity that is avoided by the use of a softer potential,[13] as has become common practice in free energy calculations.[13]

Small variations of B around the selected cavity value gave the free energy, which is calculated as

$$\Delta G_{cav}(B_i \rightarrow B_i + \delta B) = -k_B T \ln\left\langle \exp\left(-\frac{1}{k_B T} \sum_k^{\#atoms} \frac{(B_i + \delta B)^{12} - B_i^{12}}{r_k^{12}} \right) \right\rangle_i \tag{2}$$

where the energy is calculated at one of the reference B_i values over the ensemble of particles in the unperturbed state i with small perturbations δB along the trajectory, k_B is the Boltzmann constant, and the perturbation V_p is caused by the change from B_i to $B_{ref} = B_i \pm \delta B$

$$V_p(B_{ref}) = \sum_k \Delta V_{c,k} = \sum_k^{atoms} \frac{B_{ref}^{12} - B_i^{12}}{r_k^{12}} \tag{3}$$

which was calculated at one of the reference values given above,

with k that runs over the solvent atoms. The various $V_p(B_{ref})$ must connect adiabatically for δB values both positive and negative. This requirement is implicit in the definition of the cavity energy as reversible work, and in the free energy perturbation model. The δB were set to multiples of 0.0032 Å, which generated 25 perturbation points between pairs of trajectories in the region where the potential of eq 1 was used. In the initial domain, where eq 2 was used, δB was scaled down as needed. Because of the nature of eq 3, there is a redundancy of values of V_p and of the associated ΔG_{cav}, around a given B_i. This overlapping spheres approach is the same as that of Postma et al., ref 7. In practice, every simulation generates a very large spreadsheet 51*75000 (that is the perturbation for 75 ps). Overly large interactions of the perturbed cavity with the solvent molecules may occur at the edges. A procedure was then set up so that, to consider a given point in time, we require that at least one $-2k_BT < \Delta G < 2k_BT$. Because there are 25 ways to connect any two subsequent reference states (or cavities), this always happens and we never failed to find a whole series of satisfactory data. We employ a violation rate of the $2k_BT$ criterion of 1% (maximum), which becomes significant only at the edges of the domain. We realize that the $2k_BT$ value is somewhat arbitrary, but it is an operational, rather than a physically related, value.

The final $\Delta G(B)$ is the sum over the successive incremental ΔG values with cavity radii smaller than B.

The analytical expression of the free energy of cavity formation given by Pierotti reads

$$\Delta G_{cav} = K_0 + K_1 r_B + K_2 r_B^2 + K_3 r_B^3 \qquad (4)$$

where $r_B = (a + a_2)/2$ is the cavity radius given by half the sum of the solvent hard-sphere diameter, a, and the solute hard-sphere diameter, a_2, $y = \pi a^3 \rho/6$ is the volume fraction of the solvent spheres. The values of k_1, k_2, and k_3 depend on ρ, the number density of the pure solvent, and p, the pressure. Notice that r_B and B_i for many practical purposes coincide. However, the former describes the cavity when the solute is present, while the latter is used in the FEP calculations where the "bubble" of vacuum is blown up inside the solvent.

Results and Discussion

The set of plots in Figure 1 shows the PE and FEP free energies of cavity formation for the 12 solvents investigated here (acetone, **1**, cyclohexane, **2**, ethanol, **3**, toluene, **4**, chlorobenzene, **5**, benzene, **6**, tetrachloromethane, **7**, dichloromethane, **8**, chloroform, **9**, mesitylene, **10**, *o*-xylene, **11**, tetrahydrofuran, **12**). The figures show also the subsequent extrapolations of FEP and the trends obtained using surface tension, ST. One should be aware of the fact that while other approaches are presently available, PE and ST seem to be the most commonly used to calculate ΔG_{cav} in a number of quantum chemical programs. The comparisons given in Figure 1 should therefore provide an estimate of the inaccuracy that may be incurred in their use.

Consistently, PE gives lower ΔG_{cav} and there is better agreement between FEP and ST data than between FEP and PE results. To analyze further the result, and in analogy with PE, the FEP calculations were interpolated by a function with three terms up to the quadratic. Interpolation gives excellent correlation coefficients, r ≥ 0.999. The results are also shown in Figure 1. In particular, one can see that (i) for acetone, **1**, at small radii, the FEP line is intermediate between ST and PE, but it gives the lowest ΔG_{cav} from about 5 Å; (ii) for cyclohexane, **2**, the FEP curve runs parallel and slightly below the ST parabola; (iii) for ethanol, **3**, the FEP curve, after nearly coinciding with the ST line, becomes the most rapidly rising from about 3.2 Å; (iv) for toluene, **4**, the FEP curve, after nearly coinciding with the ST line, becomes the most rapidly rising from about 3 Å; (v) for chlorobenzene, **5**, the FEP curve, after nearly coinciding with the ST line, becomes the most rapidly rising from about 5 Å; (vi) for benzene, **6**, the FEP curve, after nearly coinciding with the ST line, becomes the most rapidly rising from about 5 Å; (vii) for tetrachloromethane, **7**, the FEP curve runs parallel and slightly below the ST parabola; (viii) for dichloromethane, **8**, at small radii, the FEP line is intermediate between ST and PE, but it gives the lowest ΔG_{cav} from about 6 Å; (ix) for chloroform, **9**, the FEP curve runs parallel and slightly below the ST parabola; (x) for mesitylene, **10**, the FEP curve, after nearly coinciding with the ST line, becomes the most rapidly rising from about 3.8 Å; (xi) for *o*-xylene, **11**, the FEP curve, after nearly coinciding with the ST line, becomes the most rapidly rising from about 4 Å, (xii) for tetrahydrofuran, **12**, at small radii, the FEP line is intermediate between ST and PE, but it gives the lowest ΔG_{cav} from about 4.5 Å.

TABLE 1: Coefficients of the Fits of the FEP Calculations[a]

	k_0	k_1	k_2	$a/2^b$
1	0.048; 2.350	−0.278; −2.309	0.296; 0.620; 0.406	2.380
2	0.198; 3.649	−0.654; −2.973	0.529; 0.651; 0.446	2.815
3	0.317; 2.092	−0.907; −2.256	0.662; 0.668; 0.397	2.180
4	0.485; 3.994	−1.273; −3.237	0.863; 0.703; 0.503	2.820
5	0.496; 4.303	−1.258; −3.495	0.813; 0.759; 0.597	2.805
6	0.353; 3.514	−0.972; −3.070	0.688; 0.722; 0.510	2.630
7	0.713; 3.137	−1.419; −2.697	0.680; 0.627; 0.478	2.685
8	0.287; 2.568	−0.732; −2.635	0.478; 0.736; 0.492	2.270
9	0.492; 1.445	−1.068; −1.395	0.578; 0.376; 0.482	2.480
10	0.455; 6.056	−1.198; −4.255	0.810; 0.790; 0.502	3.200
11	0.398; 5.229	−1.151; −3.927	0.833; 0.783; 0.538	3.010
12	0.038; 3.563	−0.250; −3.196	0.282; 0.771; 0.477	2.560
13	0.823; 1.321	−2.034; −2.269	1.283; 1.093; 1.302	1.400

[a] After the first semicolon, PE values obtained with standard solvent radii (given in the last column); after the second semicolon, the surface tension data[14] in appropriate units for direct comparison. All data can be used in eq 4 (limited to second order), with radii in Å and ΔG_{cav} in kcal/mol. Water, **13**, is added to the twelve organic solvents studied here for sake of further comparison. [b] For *o*-xylene and mesitylene the radius is obtained from toluene adding once or twice the difference of radii between toluene and benzene.

Empirically, one can group the 12 solvents into 3 sets: (i) acetone, dichloromethane, and tetrahydrofuran where FEP shows that ΔG_{cav} is lower than both ST and PE, (ii) cyclohexane and chloroform where FEP and ST run nearly parallel, (iii) the other solvents, where ΔG_{cav} rapidly becomes larger than what both ST and PE predict.

The three coefficients obtained from the interpolation can be compared to those of PE obtained with standard molecular radii (see Table 1). Both k_0 and k_1 fitted from the FEP data are consistently smaller than those of PE, a feature that agrees with the intuitive notion that, at zero radius, ΔG_{cav} must be zero, but also hints at a possible inaccuracy of PE. In particular, the largest (smallest) deviation for k_0 is observed for tetrahydrofuran (chloroform); while the largest (smallest) deviation for k_1 is found again for tetrahydrofuran (dichloromethane). The variations of the values of k_0 and k_1 are up to 2 orders of magnitude. The agreement between the present data and PE is only qualitatively restored, considering that in both approaches all k_1 values are negative. Substantial care must therefore be exerted with PE in the region of small radii, where the two terms play an important role in determining the value of ΔG_{cav}.

TABLE 2: Comparison of ΔG_{cav}, kcal mol^{-1}, of 11 Alkanes in Water

alkane	ref 15	present work[a]
methane	6.7	8.2
ethane	8.9	10.8
propane	11.4	13.0
butane	13.4	15.1
pentane	15.5	17.1
hexane	18.0	19.1
isobutane	13.1	14.9
2-methylbutane	15.6	16.6
neopentane	15.2	16.6
cyclopentane	14.4	15.7
cyclohexane	15.7	17.1

[a] The radius of the spherical cavity is obtained from the volumes given in Table 1, ref 15.

A feature that must be mentioned is that the FEP values of k_0 and k_1 set at $r \geq 1.2$ Å the cavity radius that requires an increase of ΔG for its formation. Any solute is likely to be larger than this limiting value and smaller "bubbles" might nearly be considered fluctuations of density.

For sufficiently large values of the cavity radius, the contribution of the quadratic term becomes dominant and, implicitly, ΔG_{cav} scales with the surface area of the cavity. Aside from the FEP and PE, Table 1 shows, for comparison, the coefficients one would obtain from the use of surface tension data. It appears that the use of the surface tensions provides "k_2" values that are rather similar to those obtained by the fits and in several cases in closer agreement than those obtained using PE. Possible exceptions are toluene, chlorobenzene, benzene, tetrachloromethane, mesitylene, and *o*-xylene. However, the set of data in Figure 1 shows that the overall agreement between FEP and PE data remains poor. It is therefore suggested that when better accuracy is required, for instance, in quantum chemical applications, the numerical values of k_i obtained from the FEP calculations could be used.

As far as we know, explicit comparison with previous data can only be carried out for alkanes in water. Gallicchio et al.[15] reported the hydration free energies of 11 alkane cavities. They also provided the alkane volumes from which one can straight-

TABLE 3: Comparison of the Calculated ΔG_{cav}, kcal mol^{-1}, and the Experimental ΔG_{solv}, kcal mol^{-1},[17] for Several Solvents and Solutes[a]

solute	volume	radius	ΔG_{cav} (γ)	ΔG_{cav} (FEP)	ΔG_{solv} (exp.)	solute	volume	radius	ΔG_{cav} (γ)	ΔG_{cav} (FEP)	ΔG_{solv} (exp.)
solvent cyclohexane						solvent ethanol					
n-octane	147.3	3.2761	3.3	3.7	−5.6	*n*-octane	147.3	3.2761	2.9	4.5	−4.2
c-hexane	102.0	2.8980	2.5	2.8	−4.4	toluene	98.8	2.8678	2.2	3.2	−4.6
benzene	80.4	2.6771	2.2	2.2	−4.2	dioxane	77.4	2.6435	1.9	2.6	−4.7
o-xylene	117.4	3.0375	2.8	3.1	−5.5	2-butanone	81.9	2.6936	1.9	2.7	−4.3
methanol	36.0	2.0490	1.3	1.1	−1.3	chlorobenzene	96.0	2.8402	2.2	3.1	−3.3
phenole	89.3	2.7731	2.3	2.5	−5.6	solvent tetrahydrofuran					
3-pentanone	98.8	2.8678	2.5	2.7	−4.3	*n*-octane	147.3	3.2761	3.4	2.3	−5.4
methyl-propanoate	87.7	2.7559	2.3	2.4	−3.7	toluene	98.8	2.8678	2.6	1.6	−5.5
2-methyl-pyridine	94.1	2.8221	2.4	2.6	−5.1	dioxane	77.4	2.6435	2.2	1.4	−5.2
nitrobenzene	102.6	2.9043	2.5	2.8	−6.6	2-butanone	81.9	2.6936	2.3	1.4	−4.5
solvent benzene						ethanol	53.0	2.3297	1.7	1.0	−4.6
n-octane	147.3	3.2761	3.7	4.6	−5.4	solvent chloroform					
c-hexane	102.0	2.8980	2.9	3.3	−4.1	*n*-octane	147.3	3.2761	3.6	3.2	−5.3
benzene	80.4	2.6771	2.5	2.7	−4.6	2-butanone	81.9	2.6936	2.4	1.8	−5.4
toluene	98.8	2.8678	2.9	3.2	−5.3	benzene	80.4	2.6771	2.4	1.8	−4.6
methanol	36.0	2.0490	1.5	1.3	−2.6	toluene	98.8	2.8678	2.7	2.2	−5.5
phenole	89.3	2.7731	2.7	3.0	−7.1	methanol	36.0	2.0490	1.4	0.7	−3.3
2-pentanone	98.8	2.8678	2.9	3.2	−5.1	phenole	89.3	2.7731	2.6	2.0	−7.1
methyl-propanoate	87.7	2.7559	2.7	2.9	−4.6	piperidine	98.3	2.8630	2.7	2.2	−6.4
2-methyl-pyridine	94.1	2.8221	2.8	3.1	−5.9	methyl-propanoate	87.7	2.7559	2.5	1.9	−4.2
nitrobenzene	102.6	2.9043	2.9	3.3	−7.6	pyridine	75.6	2.6225	2.3	1.7	−6.5
solvent toluene						aniline	93.7	2.8171	2.6	2.1	−7.3
n-octane	147.3	3.2761	3.7	5.6	−5.4	solvent chlorobenzene					
2-butanone	81.9	2.6936	2.5	3.3	−4.3	*n*-octane	147.3	3.2761	4.3	5.1	−5.2
2-pentanone	98.8	2.8678	2.8	3.9	−5.0	2-butanone	81.9	2.6936	3.0	3.0	−4.5
2-heptanone	132.8	3.1653	3.4	5.1	−6.3	propanol	70.4	2.5615	2.7	2.6	−3.8
methanol	36.0	2.0490	1.4	1.5	−2.2	toluene	98.8	2.8678	3.3	3.6	−5.2
phenole	89.3	2.7731	2.6	3.6	−6.9	methanol	36.0	2.0490	1.7	1.3	−2.4
methyl-benzoate	122.7	3.0827	3.3	4.8	−8.0	phenole	89.3	2.7731	3.1	3.3	−7.0
methyl-propanoate	87.7	2.7559	2.6	3.5	−4.6	dioxane	77.4	2.6435	2.8	2.9	−5.1
pyridine	75.6	2.6225	2.4	3.1	−5.1	methyl-propanoate	87.7	2.7559	3.1	3.2	−4.6
aniline	93.7	2.8171	2.7	3.8	−6.7	ammonia	22.9	1.7620	1.3	0.8	−1.2
solvent *o*-xylene						aniline	93.7	2.8171	3.2	3.4	−7.3
n-octane	147.3	3.2761	3.9	5.6	−5.3	solvent water					
2-butanone	81.9	2.6936	2.6	3.3	−4.2	*n*-octane	147.3	3.2761	9.4	7.9	2.9
2-pentanone	98.8	2.8678	3.0	4.0	−4.9	2-butanone	81.9	2.6936	6.4	4.7	−3.6
2-heptanone	132.8	3.1653	3.6	5.1	−6.2	propanol	70.4	2.5615	5.8	4.0	−4.8
methanol	36.0	2.0490	1.5	1.5	−1.7	toluene	98.8	2.8678	5.5	7.2	−0.9
phenol	89.3	2.7731	2.8	3.6	−6.8	methanol	36.0	2.0490	3.7	2.0	−5.1
piperidine	98.3	2.8630	3.0	3.9	−5.2	phenole	89.3	2.7731	6.8	5.1	−6.6
methyl-propanoate	87.7	2.7559	2.8	3.6	−4.2	dioxane	77.4	2.6435	6.1	4.4	−5.1
pyridine	75.6	2.6225	2.5	3.1	−5.1	methyl-propanoate	87.7	2.7559	6.7	5.0	−2.9
aniline	93.7	2.8171	2.9	3.8	−6.1	ammonia	22.9	1.7620	2.7	1.2	−4.3
solvent mesitylene						aniline	93.7	2.8171	7.0	5.3	−5.5
2-butanone	81.9	2.6936	2.5	3.1	−4.0						
2-pentanone	98.8	2.8678	2.9	3.7	−4.8						
2-heptanone	132.8	3.1653	3.5	4.8	−6.0						
3,3-dimethylbutanone	115.4	3.0231	3.2	4.2	−4.8						
phenol	89.3	2.7731	2.7	3.4	−6.8						

[a] The van der Waals volumes of the solvents, Å^3 (from ref 16) were used to obtain the effective solute radii, Å. The surface tensions of the solvents, γ, are from ref 14.

forwardly obtain the spherical radius. Table 2 shows that the agreement between the previous and the present data is within 20%.

The calculations also offer the opportunity to evaluate systematically the ratio of the caviation free energy with respect to the solvation energy. To this end, a set of van der Waals volumes were taken from ref 16 and the spherical radius for the corresponding cavity value was calculated. We then used both the free energy perturbation results and the data from the fits to calculate ΔG_{cav} for nearly one hundred solvent−solute cases, see Table 3 where we also compare the results with experimental ΔG_{solv}.[17]

For relatively small solutes we find that (i) the ΔG_{cav} from the fits of the simulations and the use of the surface tension tends to be rather similar, with the largest difference, in rare cases, reaching 50%; (ii) ΔG_{cav} has an energy cost that ranges between 50 and 100% of the total experimental ΔG_{solv}. Implicitly, this means that for these solutes, Coulomb and van der Waals terms are, in absolute value, 2−3 times larger than the free energy of cavity formation.

Conclusion

In conclusion, appraisal of the energy required to create a cavity in a liquid enters the description of important phenomena such as solvation and the formation of bubbles, whose chemistry and physics are now in development.[18] A substantial amount of work has been already carried out in the past to investigate phenomena related to the formation of cavities. Here we have shown that for 12 liquids of common use as solvents ΔG_{cav} can be calculated from a FEP procedure. The data follow more closely those obtained evaluating the surface tension of the cavity rather than the ΔG_{cav} obtained with PE. On average, on a sample of nearly 100 solvent−solute pairs, the absolute value of the cavitation free energy calculated here is 2−3 time smaller than the total solvation energy (and opposite in sign). Numerical simulations of the type presented here remain one of the safest and most direct approaches to the evaluation of ΔG_{cav}.

Acknowledgment. S.H. gratefully acknowledges supercomputing support from the University of Linz, GUP, Dr. Kranzlmüller, and Prof. Volkert, as well as University of Salzburg, RIST++, Prof. Zinterhof. S.H. present address: Novartis Research Center, Vienna, Brunner Strasse 59, A-1235 Vienna, Austria; e-mail siegfried.hoefinger@pharma.novartis.com, fax +43 1 86634727.

References and Notes

(1) Pierotti, R. A. *Chem. Rev.* **1976**, *76*, 717.
(2) Cramer, C. J.; Truhlar, D. G. *Science* **1992**, *256*, 213−217. Hawkins, G. D.; Cramer, C. J.; Truhlar, D. G. *J. Phys. Chem. B* **1997**, *101*, 7147−7157.
(3) Pohorille, A.; Pratt, L. R. *J. Am. Chem. Soc.* **1990**, *112*, 5066−5074. Pratt, L. R.; Pohorille, A. *Proc. Natl. Acad. Sci. U.S.A.* **1992**, *89*, 2995−2999. Pratt, L. R. *Annu. Rev. Phys. Chem.* **2002**, *53*, 409−436.
(4) Hummer, G.; Garde, S.; Garcia, A. E.; Pohorille, A.; Pratt, L. R. *Proc. Natl. Acad. Sci. U.S.A.* **1996**, *93*, 8951−8955.
(5) Ashbaugh, H. S.; Paulaitis, M. E. *J. Am. Chem. Soc.* **2001**, *123*, 10721−10728.
(6) Floris, F. M.; Selmi, M.; Tani, A.; Tomasi J. *J. Chem. Phys. B*, I, *16*, 6353−6365.
(7) Postma, P. M.; Berendsen, H. J. C.; Haak, J. R. *Faraday Symp. Chem. Soc.* **1982**, *17*, 55−67.
(8) Höfinger, S.; Zerbetto, F. *Chem. Eur. J.* **2003**, *9*, 566−569.
(9) Stillinger, F. H. *J. Solution Chem.* **1973**, *2*, 141−158.
(10) (a) Ponder, J. W.; Richards, F. *J. Comput. Chem.* **1987**, *8*, 1016−1024. (b) Kundrot, C.; Ponder, J. W.; Richards, F. *J. Comput. Chem.* **1991**, *12*, 402−409. (c) Dudek, M. J.; Ponder, J. W.; *J. Comput. Chem.* **1995**, *16*, 791−816.
(11) (a) Bermudez, V.; Capron, N.; Gase, T.; Gatti, F. G.; Kajzar, F.; Leigh, D. A.; Zerbetto, F.; Zhang, S. *Nature* **2000**, *406*, 608−611. (b) Cavallini, M.; Lazzaroni, R.; Zamboni, R.; Biscarini, F.; Timpel, D.; Zerbetto, F.; Clarkson, G. J.; Leigh, D. A. *J. Phys. Chem. B* **2001**, *105*, 10826−10830. (c) Biscarini, F.; Cavallini, M.; Leigh, D. A.; León, S.; Teat, S. J.; Wong, J. K. W.; Zerbetto, F. *J. Am. Chem. Soc.* **2002**, *124*, 225−233.
(12) Lii, J.-H.; Allinger, N. L. *J. Comput. Chem.* **1998**, *19*, 1001−1016.
(13) (a) Beutler, T. C.; Mark, A. E.; van Schaik, R. C.; Gerber, P. R.; van Gunsteren, W. F. *Chem. Phys. Lett.* **1994**, *222*, 529−539. (b) Simonson, T. *Mol. Phys.* **1993**, *80*, 441−447. (c) Simonson, T.; Archontis, G.; Karplus, M. *Acc. Chem. Res.* **2002**, *35*, 430−437.
(14) Jasper, J. J. *J. Phys. Chem. Ref. Data* **1972**, *1*, 841.
(15) Gallicchio, E.; Kubo, M. M.; Levy, R. M. *J. Phys. Chem. B* **2000**, *104*, 6271−6285.
(16) Marcus, Y. *The Properties of Solvents*; Wiley Series in Solution Chemistry; J. Wiley: New York, 1998; Vol. 4.
(17) Zhu, T.; Li, J.; Hawkins, G. D.; Cramer, C. J.; Truhlar, D. G. *J. Chem. Phys.* **1998**, *109*, 9117−9133.
(18) Didenko, Y. T.; Suslick K. S. *Nature* **2002**, *418*, 394−397. Attard, P.; Moody, M. P.; Tyrrell, J. W. G. *Physica A* **2002**, *314*, 696−705. Xiao, C.; Heyes, D. M.; Powles, J. G. *Mol. Phys.* **2002**, *100*, 3451−3468.